INVESTIGATION OF CO-CURRENT AND COUNTER-CURRENT SPONTANEOUS IMBIBITI

ON USING MICRO-COMPUTERIZED TOMOGRAPHY

Nayef Alyafei[1], Theis Sølling[2], and Martin J. Blunt[1]

[1] Department of Earth Science and Engineering, Imperial College London, SW7 2AZ

[2] Maersk Oil Research and Technology Centre, Qatar

This paper was prepared for presentation at the International Symposium of the Society of Core Analysts held in Avignon, France, 8-11 September, 2014

ABSTRACT
Spontaneous imbibition is an important recovery mechanism and can occur in either co-current or counter-current modes. In this paper, we study benchmark Berea sandstone and we perform imbibition experiments at ambient conditions (room temperature and atmospheric pressure). We use synthetic brine as the wetting phase and air as the non-wetting phase. By using micro-computerized tomography, we measure accurate saturation profiles across the length of the core. We compare the saturation profiles of both co-current and counter-current spontaneous imbibition, and we find them to match each other. This can be compared to the theory of the analytical solution of capillary dominated flow of co-current and counter-current spontaneous imbibition, Schmid *et al.* 2011 [1]. The solution indicates that the difference between the co-current and counter-current flow is the Buckley-Leverett fractional flow term in the co-current analytical solution. For our experiment, we use brine/air as indicated with a viscosity ratio of above 500 thus making the fractional flow approximately zero. Hence, the profile of both co-current and counter-current will be the same.

INTRODUCTION
With half the world's conventional hydrocarbons being in fractured reservoirs, spontaneous water imbibition is one of the most important recovery mechanisms for these fields [2,3]. Spontaneous imbibition can occur in two different modes: co-current and counter-current. Co-current is when the wetting phase and the non-wetting phase flow in the same direction, while counter-current occurs when the wetting phase and the non-wetting phase flow in opposite directions from the same inlet. There are many examples of spontaneous imbibition from our daily life, for example when tissue paper soaks water even without applying any force or wood absorbs paint. Similarly, water-wet rocks can imbibe water and displace hydrocarbons naturally. This is more efficient in fractured

reservoirs where we have fractures with high permeability [4]. In addition, imbibition is the process rendering the non-wetting phase to be immobile in the pore space which is optimum for carbon dioxide (CO_2) sequestration [5,6].

Micro-CT is a non-destructive technique which has recently emerged in the petroleum industry to enhance our understanding of fluid flow in porous media [7]. Current studies have shown accurate monitoring and visualisation of multiphase displacement in porous media [6-9].

In this paper, we use micro-CT to monitor the saturation profile of co-current and counter-current spontaneous imbibition in strongly water-wet Berea sandstone. We then compare the results to the theory of the newly derived analytical solution for capillary dominated flow by Schmid *et al.* 2011 [1].

EXPERIMENTAL METHODOLOGY

Tomographic datasets were obtained and analysed using the micro-CT facility built at Australian National University (ANU) and housed at the newly established digital core laboratory at Maersk Oil Research and Technology Centre, Qatar. We have conducted CT scans on a 5 mm Berea plug with absolute permeability of 72 md and porosity of 19.9% [10]. The plugs were mounted in an anodized aluminium sample holder, of inner diameter 5 mm. The holder was scanned through the aluminium-filtered (3 mm) Bremsstrahlung from the polychromatic X-ray source, operated at 80 kV and 110 mA settings. Radiographs (2048×2048 $pixel^2$) were captured by a flat panel detector. The imbibition scans inevitably need to be fast for the sampling to capture the process and a low S/N will result. They were performed using a circular trajectory, in which 720 projections were acquired, at a source-camera distance of 354 mm. The plug was imaged in a circular scan which rise to a 2.6 mm vertical reconstructed height with a 2.9 µm voxel size. Firstly, we imaged with a closed end in a dry state and with brine (consisting of 5 wt.% NaCl and 1 wt.% KCl in deionised water) on top of the plug for counter-current flow. Secondly, an experiment was performed in the same manner but with an open end for co-current flow. Each tomogram took about 1.5 hours to acquire. The high S/N scans were performed as double helical scans in which 2520 projections were acquired over the helical pitch, at a source-camera distance of 354 mm. Each of these tomograms took about 18 hours to acquire. All scans were performed at room temperature and atmospheric pressure.

IMAGE PROCESSING

First, we register the dry image to the imbibed image to make sure we have a consistent comparison between the two datasets. After that, we crop the images into circular shapes to remove the sleeve and any inconsistent backgrounds. Then, we filter the images to minimise the noise which might affect our segmentation process by using a bilateral filter [11]. This filter smooths the image without altering its morphology. After that, the images were segment according to the variation of CT contrast between phases using multi-thresholding based on Otsu's algorithm [12]. For the dry scan, we segment the image into three phases, the rock grain, the pore space, and the clays. For the imbibed image, we segment for four phases the rock grain, the pore space, the clays, the air phase, and the brine phase (Figure 1). In order to find the water saturation profile: we first, measure the porosity in each slice from the dry image. Then, we measure the gas fraction (black colour) since it is easier to detect and we divide by the porosity area fraction from the dry scans thus we find the gas saturation (S_g) across each slice. If we take one minus the gas saturation, we find the water saturation (S_w). We have 905 and 888 slices each one spaced by 2.9 µm for the co-current and counter-current respectively.

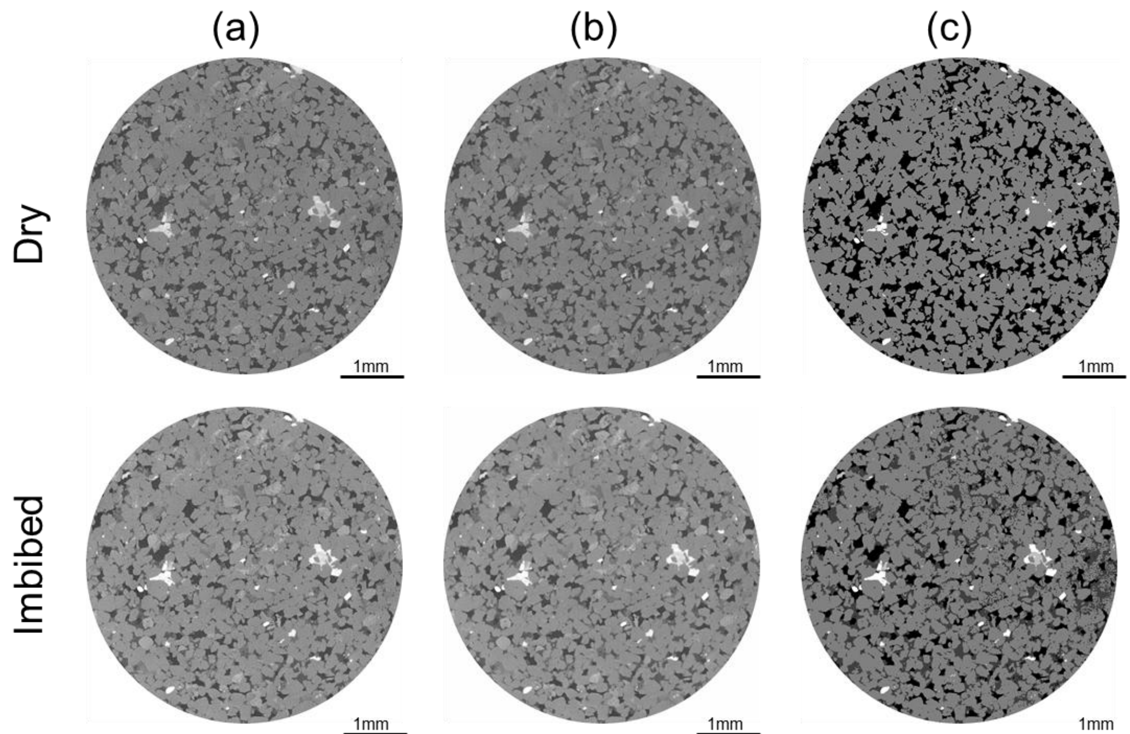

Figure 1. Image processing process: for the dry core, we first crop a subsection from the data set (a), then we filter the image using bilateral filter (b), and then we segment the image into three phases consisting of rock grain (grey), void space/air (black), and clay (white). For the imbibed image, we first register the image to the dry image and we crop the exact subsection to dry (a), then we filter the dataset by using a bilateral filter (b), and then we segment the image into four phases where in this case we have the addition of brine (dark grey) (c).

ANALYTICAL SOLUTION

We use the newly derived analytical solution for capillary dominated flow by Schmid *et al.* 2011 [1]:

$$(F - f)F'' = -\frac{\phi}{2C^2}D \qquad \text{(for co-current flow)}$$

$FF'' = -\frac{\phi}{2C^2}D$ (for counter-current flow)

where

$$D = \frac{k\lambda_w\lambda_g}{\lambda_t}\frac{\partial P_c}{\partial x}$$

is a non-linear diffusion coefficient [m^2/s], *F* is the capillary dominated fractional flow, ϕ is the porosity, *C* is a constant that quantifies the rock's ability to imbibe [m/√s], f is the Buckley-Leverett fractional flow, λ_w is the water mobility [1/Pa.s], λ_g is the gas mobility [1/Pa.s], λ_t is the total mobility [1/Pa.s], and $\partial P_c/\partial x$ is the pressure gradient [Pa/m].

Schmid *et al*. 2011 presents a formal solution to the co-current as:

$$F = \iint -\frac{\phi}{2C^2}\frac{D}{(F-f)}d^2S_w$$

and similarly with *f* =0 for counter-current flow. This equation is implicit in *F* and so can only be solved iteratively.

RESULTS AND DISCUSION

Figure 2 shows the saturation profile for co-current and counter-current flow. We can see that in both cases, the profiles are matching each other with average residual gas saturation (S_{gr}) of 0.32, Table 1. These results can be explained from the analytical solution with the only difference between the two solutions is the addition of the Buckley-Leverett fractional flow term in the co-current flow defined by:

$$f = \frac{\frac{k_{rw}}{\mu_w}}{\frac{k_{rw}}{\mu_w} + \frac{k_{rg}}{\mu_g}}$$

where k_{rw} is water relative permeability, μ_w is water viscosity, k_{rg} is gas relative permeability, and μ_g is gas viscosity.

This term will be ≈0 due to the high viscosity ratio of brine/air (μ_w/μ_g> 500); hence, making the flow behaviour of both flow modes to be exactly the same.

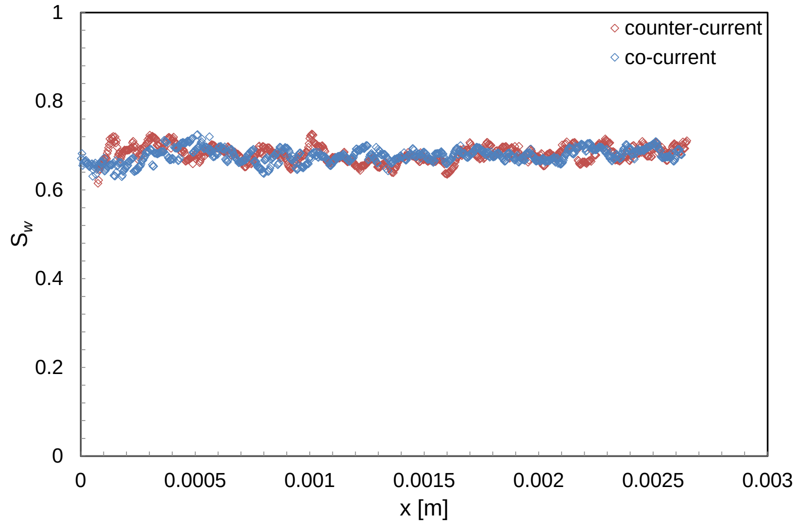

Figure 2. Saturation profile of co-current and counter-current obtained from the micro-CT data.

Table 1. Summary of the co-current and counter-current datasets, the residual gas saturation is the average value for the entire length of the sample.

Imbibition mode	Volume [voxel]	Volume [mm]	ϕ [%]	S_{gr}
Co-current	1408×1382×905	4.0×4.0×2.6	17.2	0.32
Counter-current	1244×1256×888	3.6×3.6×2.6	17.7	0.32

CONCLUSIONS

We present a micro-CT study of water saturation distribution inside a Berea rock sample. The use of the micro-CT gives accurate quantification and distribution of the saturations inside the rock. In our study, we analysed the two spontaneous imbibition modes (co-current and counter-current flow) where we had one end open (counter-current) and two ends open (co-current) and we scanned the rock after the imbibition process had elapsed under quasi-static conditions. The saturation profile and the residual gas saturation show a match in both flow modes. This was further analysed by using the newly derived analytical solution for capillary dominated flow which is an extension of the Buckley-Leverett viscous dominated flow analytical solution. The difference between the derivations of co-current and counter-current lies within the Buckley-Leverett fractional flow in the co-current derivation, where this term is ≈0 in our case since we are using air/brine system with a very high viscosity ratio.

REFERENCES

1. Schmid, K. S. Geiger, S. and Sorbie, K., "Semianalytical Solutions for Cocurrent and Countercurrent Imbibition and Dispersion of Solutes in Immsicble Two-phase Flow." *Water Resour. Res*., (2011) 47, W02550, doi:10.1029/2010WR009686.

2. Schlumberger, 2013. Carbonate Reservoirs. [Online] Available at: http://www.slb.com/services/technical_challenges/carbonates.aspx [Accessed 01 05 2014].

3. Akin, R. and Kovseck, A., "Imbibition Studies of Low-Permeability Porous Media." Paper presented at 1999 regional meeting held in Alaska.

4. Kewen, L. and Horne, R., "Characterization of Spontaneous Water Imbibition into Gas-Saturated Rocks." *SPEJ*. 2001.

5. El-Maghraby, R. and Blunt. M. J., "Residual CO2 Trapping in Indiana Limestone", *Environ. Sci. Technol.*, (2013) 47(1), 227–233, DOI: 10.1021/es304166u.

6. Andrew, M. Bijeljic, B. and Blunt, M., "Pore-Scale Imaging of Trapped Supercritical Carbon Dioxide in Sandstone and Carbonates." *International Journal of Greenhouse Gas Control* 22 (2014)1-14.

7. Blunt, M. Bijelijc, B. Dong, H. Gharbi, O. Iglauer, S. Mostaghimi, P. Paluszny, A. and Pentland, C., "Pore-scale Imaging and Modelling." *AWR*. 2013.

8. Bhattad, P. Curtis, A. Mock, A. Turner, M. Young, B. Carnerup, A. and Knackstedt, M., "Pore Scale Insights into Estimation of Residual Gas Saturation." Paper presented at the Soc. Core Analyst. 2013.

9. Berg, S. Armstrong, R. Ott, H. Georgiadis, A, Klapp, S, Schwing, A, Neiteler, R. Brussee, N. Makurat, A. Leu, L. Enzmann, F. Schwarz, J. Wolf, M. Khan, F. Kersten, M. Irvine, S. and Stampanoni, M., "Multiphase Flow in Porous Rock Imaged Under Dynamic Flow Conditions with Fast X-ray Computed Microtomography." Paper presented at the Soc. Core Analyst. 2013.

10. Al-Menhali, A. and Krevor, S., "Pressure, Temperature and Ionic Strength effects on the Wettability of CO2-Brine-Sandstone System: Core-Scale Contact Angle Measurements." Paper presented at the Soc. Core Analyst. 2013.

11. Tomasi, C. and Manduchi, R., "Bilateral filtering for gray and color images." in Computer Vision, Sixth International Conference on IEEE, 1998, pp. 839– 846. 1998.

12. Otsu, N., "A threshold selection method from gray-level histograms." IEEE Transactions on Systems, Man, and Cybernetics, 9(1), 62–66. (1979).